# A preliminary study on removing vanadium (V) from groundwater using Fe–Mn oxide nanoparticle with different stabilizers

by

Zhen Huang

A thesis submitted to the Graduate Faculty
of Auburn University
in partial fulfillment of the requirements for
the Degree of Master of Science

Auburn, Alabama
December 15, 2019

Keywords: Vanadium, Fe-Mn oxide nanoparticles, adsorption, kinetics, isotherms, surface characteristics



Approved by

Dongye Zhao, Chair, Elton Z. and Lois G. Huff Associate Professor of Civil Engineering
Mark O. Barnett, Professor and Associate Chair of Civil Engineering
Clifford Lange, Associate Professor of Civil Engineering

## Abstract

The Vanadium $V^{5+}$ removal from water body and soil is an important issue for environmental protection and conservation. Nanoparticles as adsorption and the stabilizer against nanoaprticle aggregating have become the key problems. The study used simulated experimental method to test the effect of adsorbent Fe-Mn binary oxide nanoparticles with different stabilizers, such as water soluble starch (Starch-Fe-Mn), carboxymethyl cellulose (CMC-Fe-Mn) and no stabilizer (Bare-Fe-Mn) for removing $V^{+5}$ (10 mg/L) in groundwater, and also to study the absorption characteristic and surface acting mechanism. The results showed that Bare-Fe-Mn is more capacity for removal $V^{+5}$ than that of starch- Fe-Mn and CMC- Fe-Mn. The absorption rate of Bare-Fe-Mn, starch Fe-Mn and CMC-Fe-Mn can reach to 99% in 1h, 91% in 48hrs and 96% in 48 hrs, respectively. The $V^{+5}$ absorption processes for Fe-Mn particles with different stabilizers are more accorded with the second-order sorption kinetic model. In 25℃ temperature, V+5 equilibrium adsorption data showed the best fit to the Freundlich isotherm for Fe-Mn particles with different stabilizers. Maximum adsorption occurred at pH 7.0-7.2, Langmuir isotherm model express that the maximum $V^{+5}$ adsorption capacity was 129.87 mg/g, 120.48 mg/g and 117.65 mg/g for Bare-Fe-Mn CMC-Fe-Mn and Starch-Fe-Mn nanoparticles, respectively. The above change is related closely with pre- and post-absorbed surface features, Zeta potential, FTIR of Fe-Mn nanoparticles with different stabilizers, most important is starch and CMC coating the surface of Fe-Mn nanoparticles and decrease the $V^{+5}$ ion adsorption. Therefore, Fe-Mn oxide nanoparticles without stabilizer could be considered as an effective material for treating vanadium pollution in aqueous condition.



**Keywords:** Vanadium; Fe-Mn oxide nanoparticles; adsorption; kinetics; isotherms; surface characteristic;

## Acknowledgments

Few years ago, when I stepped onto the flight to Auburn, I told I told myself I should be a decent guy when I graduate, but, I mess it up. I spent long time stay here, however, I let all people feel despair on me cause my bad habits. I don't like talk and commutate with others people and always abandon myself to my personal world. But, I think is time to wake up, because I still need to complete some work, it called responsibility.

Firstly, I would like to express my deepest gratitude to my advisor professor Dongye Zhao. Thanks for his continuous support of my study and live, for his guidance, motivation, and patience. I'm sure I will stay in darkness if without his help.

Besides my advisor, I would like to thank my thesis committees: Dr. Mark O. Barnett, and Dr. Clifford Lange, for their support, insightful comments.

In addition, I want to thanks CSC (China Scholarship Council) and AU IGP project for funding.

Especially, I would like to thank former and current fellow students in our research group, Shuting Tian, Haodong Ji, Fan Li, and Jun Duan and so on, for their constant affection and support throughout my research and live.

Last but not least, I want to say thanks to my parents, no matter what the result it is, I still love you.

## Table of contents

## List of Tables

## List of Figures

## List of Abbreviations

| | |
|---|---|
| CMC | Carboxymethyl cellulose |
| $FeCl_2$ | Ferrous chloride |
| $KMnO_4$ | Potassium permanganate |
| SEM | Scanning electron microscope |
| FTIR | Fourier transform infrared spectroscopy |

# 1. Introduction

## 1.1. Overview

Vanadium is a transition rare metal element accounting for about 0.02-0.03% in the composition of the earth's crust (Yang, et al. 2014), and contents of soils are range from 10-220 mg/kg in soils. Vanadium is an important raw and processed material called a “metal vitamin" in the manufacturing of iron and steel, petrochemical industry, textile, rubber and other industries (Manohar, et al. 2005). It main exists in the +3, +4 and +5 oxidation states under aqueous conditions(Peacock and Sherman 2004). The most stable and toxic oxidation state of V is $V^{+5}$ ($VO_4^{3-}$). Under oxygenated groundwater conditions, $VO_4^{3-}$ can combine with other biological substances forming complexes that are easily absorbed and taken up by plants (Mandiwana and Panichev 2004; Manohar, et al. 2005). According to analysis, about 10% of groundwater samples from California contain vanadium in amounts exceeding 25 μg/$dm^3$ (Imtiaz, et al. 2015). In most of the area surrounding the Panzhihua mining area in China, the average vanadium content of the surface soil is 224 mg/kg, which is 2.79 times the soil background value.

There is evidence that $V^{+5}$ acts an activator of the enzyme function in nitrogen fixation by nitrogen-fixing soil bacterium through the partial substitution of molybdenum(Ayers and Westcot 1985; Bellenger, et al. 2008; Rehder 2015).However, excess amount of vanadium is toxic and cause various diseases, such as negative effects on liver and kidney, lung injuries and paralysis (Zhang, et al. 2014), and as a potentially dangerous pollutant in the same class as mercury, lead and arsenic (Lazaridis, et al. 2003). Vanadium has been listed in the United Nations Environment Program’s environmental risk priority element (Goulding 1989).

To mitigate human exposure to vanadium, the UN’s Food and Agriculture Organization (FAO) Food proposed the maximum allowable concentration as 0.1 mg/L in drinking water(Ayers

and Westcot 1985), some countries over the worled also make the vanadium discharge standard for vanadium industry, such as vanadium concentration 0.05 mg/L in drinking water in California, USA(Health 2010) and in China (BG3838-2000), Bureau of Indian Standards (1981) have set a limit of 0.2 mg /L vanadium in surface water, standard for vanadium intervention value in groundwater is 0.07 mg/L in Netherlands. Therefore, the removal of vanadium (V) from wastewaters is one of the most important issues for environmental protection and conservation(Anirudhan and Radhakrishnan 2010).

There are several approaches have been attempted to treat vanadium-containing wastewater, such as chemical precipitation (Parks and Edwards 2006), biological treatment(Pennesi, et al. 2013) , ion exchange(Yeom, et al. 2009), membrane filtration (Lazaridis, et al. 2003), adsorption (Kavakli, et al. 2004; Liao, et al. 2008) . Adsorption is widely used for removing vanadium because of its high efficiency. Some absorbers have been reported, such as chitosan, carboxymethyl chitosan (Wang, et al. 2011) and crosslinked chitosan (CCTS)(Qian, et al. 2004), active carbon(Dogan and Aydin 2014; Keranen, et al. 2015), melamine (Peng, et al. 2017), amine-functionalized poly (hydroxyethylmethacrylate)-grafted tamarind fruits shell (Anirudhan and Radhakrishnan 2010), metal sludge and cement (Bhatnagar, et al. 2008), and bisphosphonate nanocellulose (Sirvio, et al. 2016). There are different kind of metal or compound materials to remove V from waste water, such as $ZnCl_2$ (Namasivayam and Sangeetha 2006), zeolite-polypyrrole (MZ-PPY) (Mthombeni, et al. 2016), calcined Mg/Al hydrotalcite (Wang, et al. 2012) chitosan-zirconium(IV) composite (Zhang, et al. 2014) zeolite modified by ferrous sulfate, surface-modified montmorillonite used in mine(Oyewo, et al. 2017) activated carbon surface with iron nanoparticles (Sharififard, et al. 2017), octylamine functionalized magnetite nanoparticles (Parijaee, et al. 2014) and so on.

In recent years, the preparation of Nano iron and its applications in heavy metal pollution treatment have attract huge attention from the world (An, et al. 2011). However, the Nano particles tend to aggregate rapidly into precipitation, meanwhile, it will lose their unique advantages, such as soil deliverability and huge surface area. To deal with the problem of the nanoparticles, organic polymers are often employed, such as starch and carboxymethyl cellulose (CMC)(An, et al. 2011; He and Zhao 2005; He and Zhao 2007). Because the stabilizers can attached on the nanoparticles and prevent the particles from aggregation due to electrostatic stabilization mechanisms, which can increase stability of particles(Sharififard, et al. 2017).Some studies showed the prepared Fe-Mn nanoparticle size reached to 20-50 nm in experimental condition and surface area over 120 $m^2/g$ (He and Zhao 2007; Shan and Tong 2013). And one result showed that NaCl solution containing 300 mg/L As(III) was treated with starch-stabilized Nano iron ions, As(III) was removed completely, whereas only 20% of the As was removed from a solution in which none of the stabilizer was added (He and Zhao 2005), Column leaching tests of an As(III)-laden soil indicated that application of CMC-stabilized Fe–Mn transferred nearly all water soluble As(III) to the nanoparticle phase (An and Zhao 2012). Compared with arsenic, vanadium has similar chemical structure and valance, therefore, how does the Fe-Mn nanoparticle with different stabilizers act on vanadium adsorption, it is the experiment want to understand in this paper.

### 1.2. Goals and objectives

The main objectives of this research are as followings:

1) Compare the vanadium absorption characteristic including kinetic and equilibrium isotherm models of starch- or CMC-stabilized Fe–Mn oxide nanoparticles, and removal vanadium from water.

2) Investigate the impact factors on Fe-Mn nanoparticles adsorb vanadium, such as pH,

both substrate and stabilizers concentrations.

3) Analysis the surface character of the nanoparticles before and after adsorption of vanadium from water, and understand the mechanism of vanadium absorption by Fe-Mn nanoparticles.

## 2. Materials and methods

### 2.1 Chemical

All chemicals were used chemicals of analytical grade or higher in this research, including ferrous chloride ($FeCl_2.4H_2O$), potassium permanganate ($KMnO_4$), carboxymethyl cellulose (CMC, sodium salt, MW=90,000), and a hydrolyzed potato starch were purchased from Acros Organics (Morris Plains, NJ, USA). $Na_3V_2O_4$ and NaOH were purchased from Fisher Scientific (Pittsburgh, PA, USA). Hydrochloric acid, sulfuric acid and nitric acid were purchased from Mallinckrodt Chemical (St. Louis, MO, USA. All solutions were prepared with ultrapure deionized (DI) water (18.2 $\Omega cm^{-1}$).

### 2.2 Preparation of CMC-stabilized Fe-Mn particles

Stabilized Fe-Mn oxide nanoparticles were prepared following the redox-precipitation method by Zhang et al. (Zhang, et al. 2005) At first, a 1 wt. % starch solution was prepared by mixing 4 g of the starch powder with 400 ml DI water, then, keeping stirring with 600 rpm and heating the mixture to 100 °C on magnetic stirrer until the starch solution started boiling. After 10 mins, heating was removed and the solution retain stirring at room temperature (21 ◦ C) to 24 hours. Contrast with preparing 1 wt. % starch solution, a 1 wt. % CMC solution was prepared with same process besides heating. A desired volume (0-20mL) of a starch or CMC stock solution (1 wt.%) was added into a 200-mL glass flask containing 150 mL of an $FeCl_2$ solution and mixed for 20 min

under $N_2$ purging. Then, 20 mL of a $KMnO_4$ solution was added into the mixture with stirring, and the desired nanoparticles were obtained according to the redox reaction. Then, the pH of the mixture was adjust immediately to 7.0 using 1 M NaOH and the total volume of the mixture was adjust to 200 mL by adding DI water (0–10 mL). The resulting nanoparticle suspension contained 0.1 g/L Fe and 0.03 g/L Mn with stabilizers concentration of 0.1 wt. %( starch and CMC). For comparison, bare Fe-Mn particles were prepared in the same approach. The nanoparticles were allowed to grow for 1 to 2 hours under shaking at 200 rpm before the subsequent experiments. The stabilized nanoparticles remained fully dispersed in water as suspension, while the process of equipment need close to 6 hours. The desired nanoparticles could be obtained through the following redox reaction Eq. (1).

$$3Fe^{2+} + Mn^{7+} \rightarrow 3Fe^{3+} + Mn^{4+} \qquad (1)$$

The surface characteristics including zeta (ζ) potential, Fourier Transform Infrared (FTIR) of the pre- and post-absorption vanadium of Fe–Mn nanoparticles was analyzed. The Zeta potential (ζ) of the particles was measured with a Zeta sizer Nano ZS (Malvern Instruments, UK) at room temperature (21 ◦ C). Typically, 0.75 mL of a nanoparticle suspension of 0.1 g/L of Fe-Mn was filled in a folded-capillary cell and then measured, and all process was conduct at Auburn University civil engineering lab.

FTIR spectra were used to determine vanadium adsorption mechanisms. After prepared bare Fe-Mn nanoparticles at Auburn University civil engineering lab, the samples were vacuum-dried, and then ground in a mortar to fine powders, which were then mixed with KBr at a sample-to-KBr ratio of 5:95 by weight. The mixtures were pressed into thin films with a hydraulic press at 9 metric tons for 2 min. The specimen was then scanned and characterized using an IR Prestige-21 spectrometer (Shimadzu, Japan) over the wave number ranging from 400-4000 $cm^{-1}$ at Beijing

University in China.

### 2.3 Batch tests: adsorption, kinetics and isotherms studies

A series of batch kinetic tests were carried out to test the vanadium adsorption rate and extent using Bare and stabilized Fe–Mn nanoparticles (CMC and Starch), respectively.

The adsorption test was initiated by adding a known volume of vanadium solution into a nanoparticle suspension accord to the following experimental conditions: total suspension volume =200 mL, nanoparticle dosage = 0.1 g/L as Fe, initial vanadium concentration 10 mg/L and the pH=7.0. The mixtures were continuously mixed on a platform shaker at 200 rpm. At predetermined times, samples were taken, filtered through a 25 nm mixed cellulose esters membrane (MF-Millipore Corp., Billerica, MA, USA), which was able to completely remove the nanoparticles, but did not remove the soluble materials. The filtrates were then acidified to pH 2.0 with 1 M $HNO_3$ and analyzed for V.

All the tests were conducted in duplicates and control tests were carried out without the nanoparticles. Adsorption equilibrium tests were carried out by equilibrating the vanadium adsorption batch systems for 48 hours. To obtain the adsorption isotherms, the initial vanadium concentration spanned from 0 to 100 mg/L; to test the stabilizer effects, the concentrations of starch and CMC were varied from 0 to 0.2 wt. %;

The $V^{+5}$ removal percentage was determined by using the following equations (Parijaee, et al. 2014):

$$\% \text{ Removal} = (Co - Ce)/Co \times 100 \qquad (2)$$

Meanwhile the equilibrium sorption capacity was determined using Eq. (3):

$$qe = [(Co - Ce)/m] \times V \qquad (3)$$

Where qe is the equilibrium amount of $V^{+5}$ adsorbed per unit mass of adsorbent (mg/g), m is the sorbent mass (g), V is the sample total volume (L), Ce is the equilibrium concentration (mg/L) and Co is the initial concentration (mg/L).

The adsorption kinetics experiments were carried out in a batch reactor with initial $V^{+5}$ concentrations of 10 mg/L. A mass of 0.1 g of the sorbent was used. The reactor was continuously stirred at a speed of 250 rpm. At predetermined time intervals 0, 0.5, 1, 2, 4, 6, 12, 15, 18, 21, 24, 36, 48 hours, 5 mL sample was withdrawn from the reactor. Each sample was immediately filtered using syringe filters and the resulting filtrates were analyzed using Varian 710-ICP-OES (detection limit of 10 ug/L for V) at a wavelength of 311.84 nm to determine the vanadium residual concentration.

The amount of vanadium removed at given time was calculated using Eq. (4).

$$qt = [(C0 - Ct)/m] \times V \qquad (4)$$

Where Ct (mg/L) is the vanadium residual concentration at time t, qt (mg/g) is the time dependent amount of vanadium adsorbed per unit mass of adsorbent.

Sorption isotherm studies were carried out in a temperature controlled thermostatic shaker. 200 mL solutions of $V^{+5}$ concentration ranging from 0, 5, 10, 20, 40, 60 and 100 mg/L were contacted with 0.1 g/L Fe–Mn particles with stabilizer starch, CMC or no stabilizer (bare) treatment. The samples were shaken for 24 hrs at the temperatures 298K at 160 rpm. The experiments were performed at pH 7.0-7.2. Samples were studied in duplicates. At the end of the experiment, samples were filtered using syringe filters and the residual vanadium concentration was measured by inductively couple plasma-emission spectroscopy (ICP-OES).

It can be used Langmuir, Freundlich and Temkin models to describe quantitatively sorption isotherms:

$$\frac{C_e}{q_e} = \frac{C_e}{q_m} + \frac{1}{K_L q_m} \quad (5)$$

$$lnq_e = lnK_F + \frac{1}{n} lnC_e \quad (6)$$

$$q_e = BlnA + BlnC_e \quad (7)$$

Where $C_e$ is the equilibrium vanadium concentration in the solution (mg/L), $q_e$ is the equilibrium $V^{+5}$ sorption quantity on the sorbent (mg/L), $q_m$ is the maximum sorption capacity (mg g/L), and KL, KF, n, B and A are the equation constant.

**2.4 Vanadium absorption characteristic influenced by pH and the substrate**

The effect of pH was studied by varying the initial pH of the 200 mL solution within the range of 6–9, and contacting 10 mg/L $V^{+5}$ concentrations. For effect dosage of Fe-Mn nanoparticle, it was contacted with 0.3, 0.5, 0.7 g/L Bare-Fe–Mn particles in 200 Ml, and pH was controlled in 6-7. The samples were shaken for 24 h at varying temperatures of 298K at 160 rpm. The experiments were performed at pH 7.0-7.2. At the end of the experiment, samples were filtered using syringe filters and the residual vanadium concentration was measured by inductively couple plasma-emission spectroscopy (ICP-OES). The effect of adsorbent dosage was previously reference(Keranen, et al. 2015). For effect of stabilizers, it was used starch and CMC stabilizer in solution as 0.05, 0.1, 0.15 and 0.2 g/L, vanadium concentration is controlled in 10 mg/L, reactor volume 200mL, to equilibrium time is 24 hrs., there are no Fe-Mn nanoparticles in liquid.

**2.5 Chemical analysis**

Solution or suspension pH was measured using an Oakton pH meter (pH 510 Benchtop

Meter, Oakton, CA, USA). Vanadium was measured using an ICP- OES (710-ES, Varian, USA). And Zeta potential was analyzed using Zetasizer Nano ZS (Malvern, Instruments, UK).

## 3. Results and discussion

### 3.1 Characterization of Fe-Mn nanoparticles

#### *3.1.1 Zeta potential*

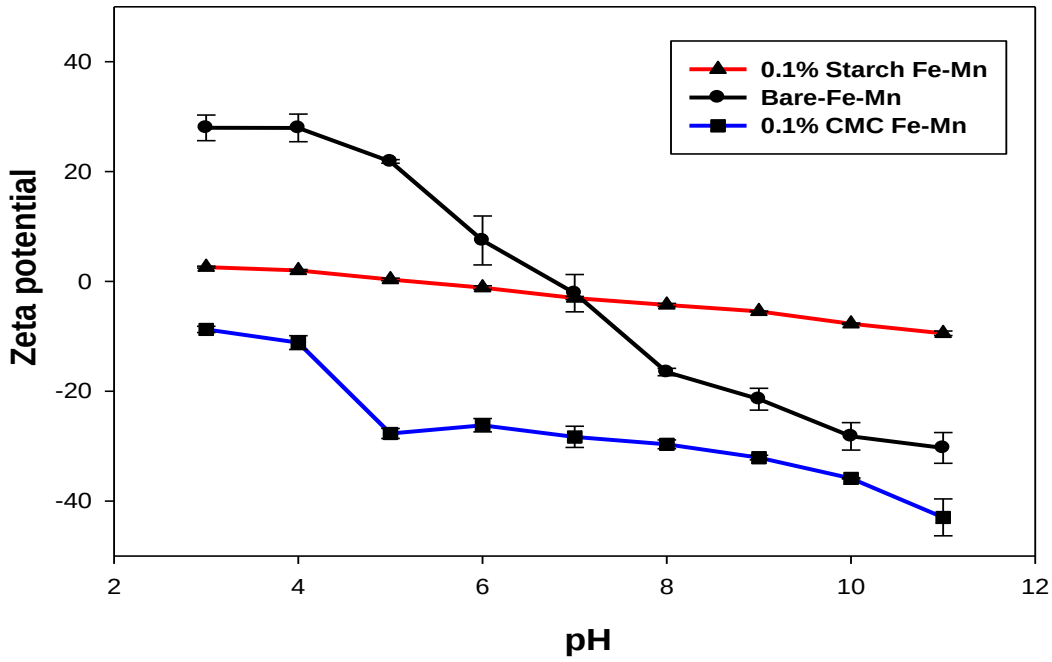


**Fig. 1.** Zeta potential as a function of pH for bare and stabilized Fe–Mn nanoparticles.

Fig. 1 shows the measured zeta potential as a function of pH for bare, CMC and starch Fe-Mn nanoparticles. It found that coating of the neutral starch molecules greatly altered the Zeta potential value over a broad pH range. For the bare Fe–Mn binary oxide nanoparticles, the Zeta potential value is a sharp change from +21.83 to −28.23 mV over the pH range of 4–10, which indicated a point of zero charge (PZC) pH of −6.8. Kosmulski et al. According to some

research(Keranen, et al. 2015), it revealed PZC values for goethite and Fe hydroxides are 8.32 and 7.99, respectively. Su and Suarez(Su and Suarez 1997) reported a PZC of 8.5 for synthetic amorphous $Fe(OH)_3$. Comparing the Zeta potential–pH profile of bare Fe–Mn and iron oxide minerals, it shows that $Fe(OH)_3$ dominates the characteristics of the Fe-Mn binary oxide nanoparticles. However, in the presence of 0.1 wt. % of starch, the surface potential was hugely shielded. Over the pH range of 5.2, it was nearly zero, and it was only changed to -10 mV when pH was increased to 11. This looks that the presence of starch that belong to a neutral polymer with dense H-bonding (Deschamps, et al. 2005; Ravishankar, et al. 1995)that provide with a strong surface "buffer" that diminishes the effect of H+/OH- on the surface charge. Evidently, for Fe–Mn particles, the starch macromolecules have pre-occupied the functional sites of the core, which hinders protonation or deprotonation of these functional groups. However, for the CMC Fe-Mn, the result show the Zeta potential tend to more negative than bare Fe-Mn. The Zeta potential value was from -9.72 mV to -44.23 mV over the pH range from 4-10. This result is very similar to the work by B. An and Zhao(An and Zhao 2012). According to the standpoint of particle stabilization, starch stabilizes particles due to steric exclusion, and CMC works through concurrent both steric and electrostatic repulsion.

### *3.1.2 FTIR analysis*

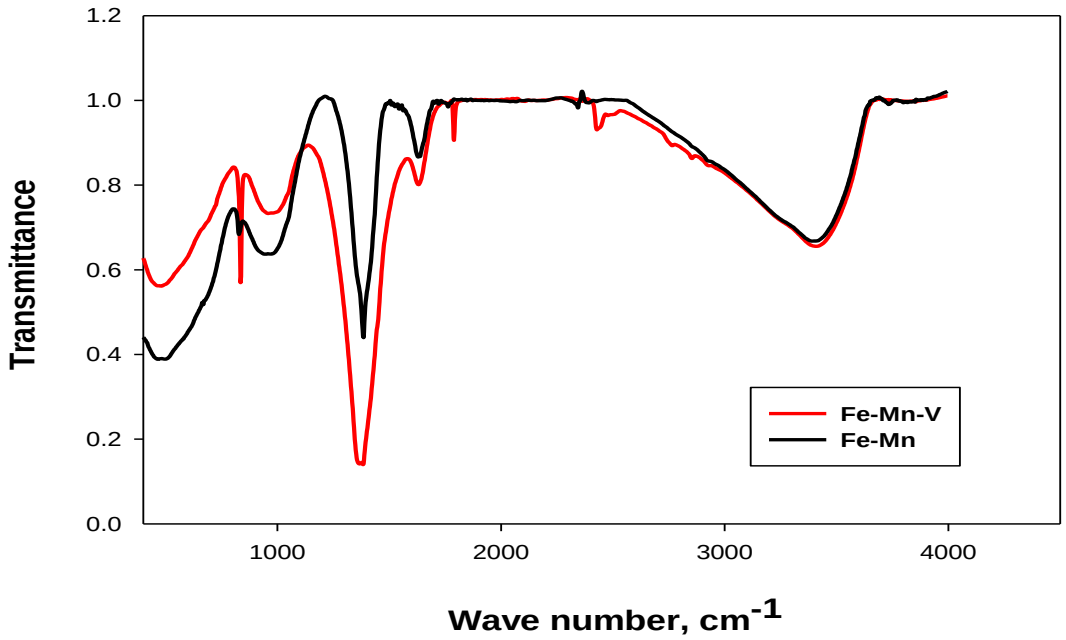


**Fig.2.** FT-IR spectrum of pre- adsorption and post- adsorption vanadium of bare Fe-Mn nanoparticles.

In order to explore the qualitative sorption characteristic of surface functional groups of Fe-Mn nanoparticles, FTIR spectra at range of 400-4000 $cm^{-1}$ were identified before and after adsorption of $V^{+5}$ onto bare Fe-Mn nanoparticles. FTIR studies of various iron oxides have been widely reported(An and Zhao 2012), such as 580 $cm^{-1}$ for magnetite, 560 $cm^{-1}$ for ferrihydrite film, 441 and 580 $cm^{-1}$ for low crystalline ferrihydrite. Two peaks at 3444 $cm^{-1}$ and 3430 $cm^{-1}$ were found for neat starch and CMC, respectively.

Fig. 2 shows the FTIR spectra of bare Fe-Mn nanoparticle before and after adsorbed $V^{+5}$. The peak at 1627 $cm^{-1}$ is corresponds to the deformation of water molecules, which reveals the presence of physisorbed water on the oxides(Zhang, et al. 2009). The peak at 2359 $cm^{-1}$ caused by strong O=C=O stretching vibrations (Namasivayam and Sangeetha 2006). There are two peaks appear at 1140 and 1234 $cm^{-1}$ respectively, which can have attributed to the vibration of hydroxyl groups of iron (hydr)oxides (Fe–OH). And the peak at 480$cm^{-1}$ corresponds to the Fe-O vibration of $Fe_3O_4$ (Keranen, et al. 2015) the presence of Mn in iron oxide reduced the band

strength of Fe-O group. Asymmetric COO- vibration occurred at 1580 $cm^{-1}$ and the 1153 $cm^{-1}$ band may have contributions from both C=O stretching and O-H bending modes in phenolic groups. The peak around 841 $cm^{-1}$ expresses characteristics of V-O stretching in the $VO_4^{3-}$. The V-O stretching peaks are contributed to the uniform regular $VO_4^{3-}$(Lim 2012). One single band with shifted wave number to 1815 $cm^{-1}$ was observed, which may express that surface complexation was the primary mechanism for bare Fe-Mn nanoparticles adsorb vanadium.

### *3.1.3 Characterization of Fe-Mn nanoparticles*

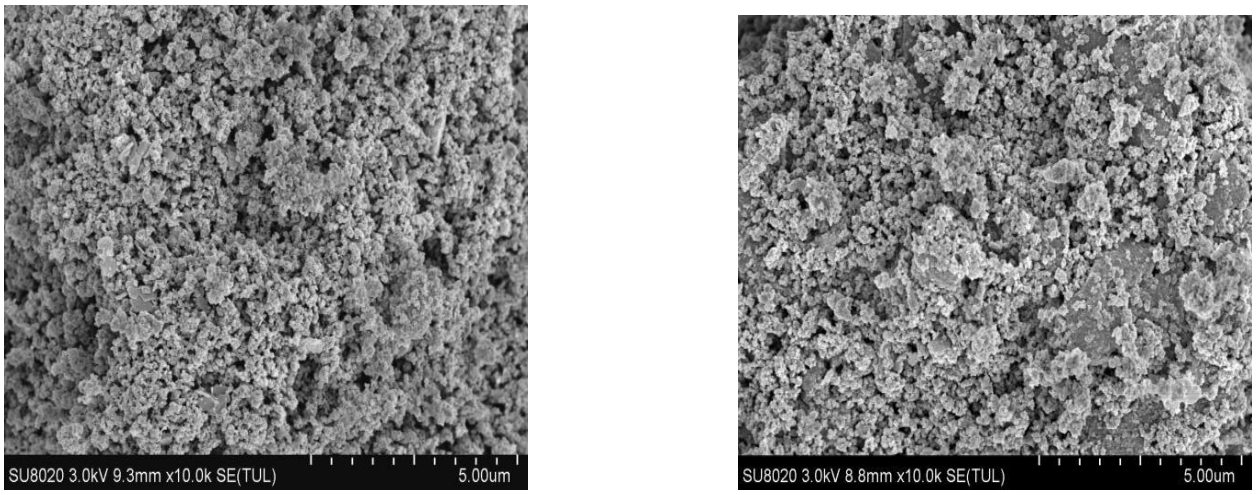


**Fig. 3.** SEM images of Bare Fe-Mn binary oxide nanoparticles treat vanadium (a) pre-adsorption (b) post-adsorption

Fig.3.shows the characterization of Bare Fe-Mn nanoparticles, the nanoparticles shows granulated condition with huge area before add vanadium; fig (b) expresses there are some crumb structures appear after adsorption and the total nanoparticles of specific surface area tend to decrease. It may suggest that the Fe-Mn nanoparticle has a capacity to adsorb vanadium from water condition.

## 3.2 Vanadium（ $V^{+5}$） adsorption characteristic and the kinetics

Fig.4.a shows the $V^{+5}$ adsorption rates of Bare Fe-Mn, Starch Fe-Mn and CMC Fe-Mn

stabilized nanoparticles. It can be found that the vanadium adsorption rate of Bare-Fe–Mn particles can reach to 99% in −1 h, and CMC-stabilized and Starch-stabilized particles 91% in and 96% in more than 48 hours, respectively. The order of equilibrium removal vanadium in water solution follows Bare-Fe-Mn particles> Starch-Fe-Mn particle > CMC-Fe-Mn particle.

Fig.4.b expressed that the $V^{+5}$ up taking amount by Bare Fe–Mn particle is higher than that of Starch-Fe-Mn and CMC-Fe-Mn particles, the $V^{+5}$ adsorption capacity for Bare-Fe-Mn, Starch-Fe-Mn and CMC-Fe-Mn particles are 19.55 mg/g, 17.55 mg/g and 18.57 m/g at pH 7.0 in experiment, respectively.

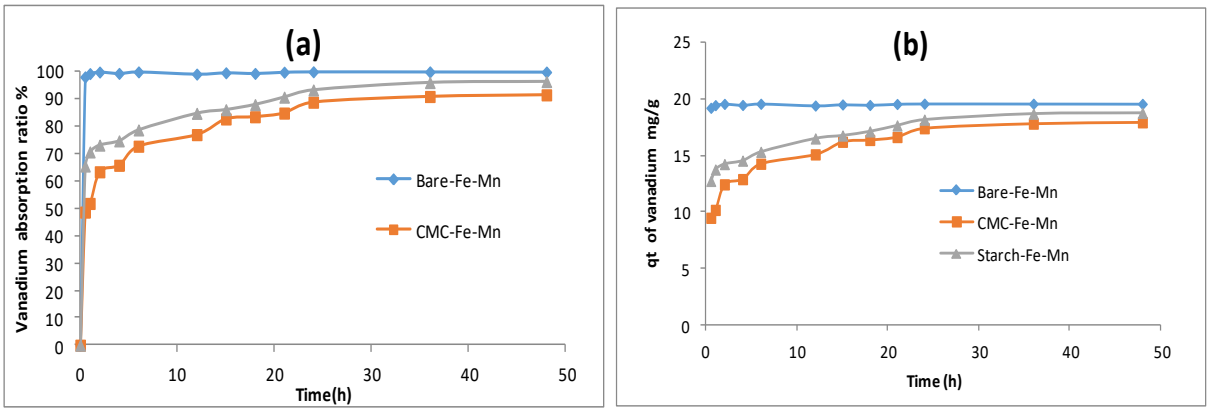


**Fig.4.** Vanadium absorption ratio (a) and absorption amount (b) by Fe-Mn oxide nanaparticles with different stabilizers. Experimental conditions: initial V = 10 mg/L, nanoparticles = 0.1 g/L as Fe, CMC or starch = 0.1 wt. %, pH = 7.0 ± 0.2 (constant**).**

Sorption kinetics of $V^{+5}$ onto Fe-Mn oxide nanoparticles with different stabilizers was analyzed using non-linear method by pseudo-first order kinetic model, pseudo-second order kinetic model and Elovich kinetic models given in equation(Dogan and Aydin 2014).

$$\ln(q_e - q_t) = \ln q_e - k_1 t \qquad (8)$$

$$t/qt = 1/k2\ qe2 + t/qe \quad (9)$$

$$q_t = \frac{1}{\beta}\ln(\alpha\beta) + \frac{1}{\beta}\ln t \quad (10)$$

Where t: time (h), $q_e$: adsorbed $V^{+5}$ amount (mg/g) in equilibrium state, $q_t$: adsorbed material amount (mg/g) in t time, k1 and k2 are the pseudo first-order and pseudo-second-order rate constants, α and β are the Elovich equation constants.

Pseudo-first-order kinetic model defined by Lagergren, the adsorption of a liquid-solid system depending on the capacity of the solid material, Eq. (8) is depended on the adsorption capacity of the solid and the concentration of the solution. Pseudo-second-order kinetic model assumes the adsorption rate is controlled by the chemisorption mechanism, and the adsorption process involves the sharing or transfer of electrons between adsorbents and adsorbents (Ho and McKay 1998) Elovich kinetic models often be used to describe chemisorption processes (Juang and Chen 1997) and the mathematics is given in Eq. (9).

The kinetic parameters are summarized in Table 1. The best describes the kinetic sorption data was assessed by considering the correlation coefficient ($R^2$). Based on the $R^2$ values, it is suggested the adsorption kinetic data is best described by the pseudo-second-order equation.

**Table 1. Kinetics parameters for $V^{+5}$ adsorption on Fe-Mn oxide nanoparticles with different stabilizers.**

| Stabilizers | Pseudo-first-order model | | | Pseudo-second-order model | | | Elovich model | | |
|---|---|---|---|---|---|---|---|---|---|
| | $q_{e \cdot exp}$ (mg/g) | $k_1(h^{-1})$ | $q_{e \cdot cal}$ (mg/g) $R^2$ | $q_{e\bullet exp}$ (mg/g) | $k_2$(g/mg•h) | $q_{e\bullet cal}$ (mg/g) $R^2$ | $\alpha$ (g/mg• | $\beta$ (g/mg | $R^2$ |

| | | | | | | | | | | | |
|---|---|---|---|---|---|---|---|---|---|---|---|
| | | | | | | | | | h) | ) | |
| Bare | 19.5798 | 0.022 | 42.9806 | 0.0187 | 19.5798 | 2.0065 | 19.5487 | 1.000 | 338.5839 | 17.4825 | 0.4462 |
| CMC | 17.9356 | 0.1024 | 11.7409 | 0.9728 | 17.9356 | 0.0393 | 17.7469 | 0.9981 | 6.7871 | 0.5083 | 0.9854 |
| Starch | 18.7683 | 0.073 | 15.4211 | 0.9850 | 18.7683 | 0.0539 | 18.5708 | 0.9982 | 7.7876 | 0.7311 | 0.9638 |

### 3.3 Adsorption isotherms

Fig.5 shows $V^{+5}$ adsorption isotherms for Bare-Fe-Mn, Starch-Fe-Mn and CMC-Fe-Mn stabilized nanoparticles. The bare Fe-Mn expresses the highest efficiency to treat high concentration vanadium, and its adsorption ability (5-100 mg/L vanadium) is equal to 129.87 mg/g. However, for CMC-stabilized Fe-Mn and starch-stabilized Fe-Mn, the $V^{+5}$ removal ability is 120.48 mg/g and 117.65 mg/g, respectively.

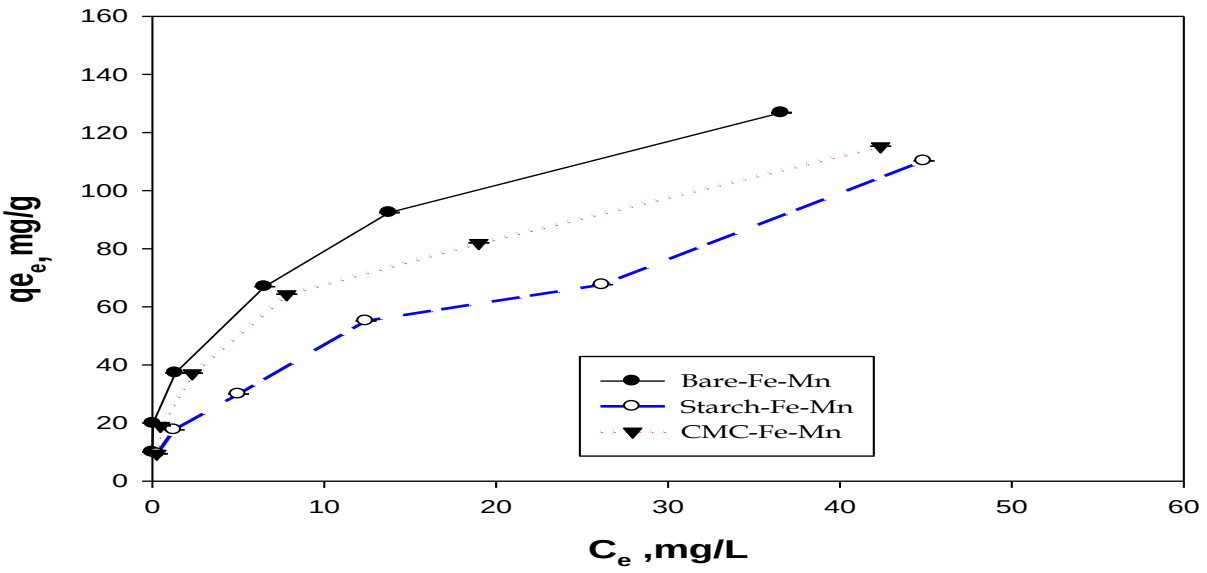


**Fig. 5.** Vanadium sorption isotherms with bare, starch- or CMC-stabilized Fe–Mn nanoparticles. Experimental conditions: Initial V = 5–100 mg/L, Nanoparticles = 0.1 g/L as Fe, CMC or starch = 0.1 wt. %, pH = 7.0 ± 0.2 (constant), Equilibrium time = 48 h

When reaching sorption equilibrium, the concentration of sorbents in bulk solution will be in dynamic balance with that in the liquid-sorbent interface. At this point, the equilibrium solution concentration remains constant. The sorption isotherm is based on the assumptions that every

sorption site is equivalent, and the ability of particles to bind there is independent of whether or not adjacent sites are occupied. In this study, Langmuir and Temkin models were used to describe quantitatively sorption isotherms and the equation constant and summarized in Table 2.

The Langmuir model suggests a monolayer adsorption, with no lateral interaction between the sorbed molecules. The Freundlich model assumes heterogeneous adsorption due to the diversity of sorption sites or the diverse nature of the metal ions adsorbed, free or hydrolyzed species. Temkin model considered the heat of adsorption of all the molecules in the layer would decrease linearly with coverage due to adsorbate / adsorbate interactions.

In the Freundlich equation, isothermal constant KF can indicate the strength of adsorbent adsorption capacity, and the stronger the KF, the stronger the adsorption capacity. The value of 1/n can be used as an index of the adsorption strength of absorbent. The n can describe the adsorption performance of adsorbent, n<1 means the adsorption is multilayer adsorption(Arias, et al. 2005)1.7% higher than that of CMC-Fe-Mn particle and Starch-Fe-Mn particle, it means that Bare-Fe-Mn particle has stronger $V^{+5}$ adsorption capacity than that of Fe-Mn particle with Starch or CMC stabilizers. On the other hand, 1/n <1 among all treatments shows that vanadium adsorption of Fe-Mn nanoparticles with different stabilizers are similar and belong to multilayer adsorption.

**Table 2. A comparison of isotherm model on Vanadium absorption by Fe-Mn oxide nanoparticles with different stabilizers.**

| stabilizers | Langmuir | | | Freundlich | | | Temkin | | |
|---|---|---|---|---|---|---|---|---|---|
| | $q_m$ | $K_L$ | $R^2$ | $K_F$ | 1/n | $R^2$ | A | B | $R^2$ |
| Bare-Fe-Mn | **129.87** | 0.3582 | 0.963 | **41.6036** | 0.2824 | 0.984 | 1.34E+25 | 0.0694 | 0.8445 |
| CMC-Fe-Mn | **120.48** | 0.0927 | 0.8706 | **15.927** | 0.4744 | 0.9879 | 1.41E+05 | 0.0464 | 0.8282 |

| | | | | | | | | | |
|---|---|---|---|---|---|---|---|---|---|
| Starch-Fe-Mn | **117.65** | 0.2673 | 0.9634 | **29.997** | 0.3203 | 0.9907 | 1.20E+18 | 0.0606 | 0.8547 |

The comparison of correlation coefficients values ($R^2$) of the linearzed form of Langmuir, Freundlich and Temkin models cleared that $R^2$ in Freundlich model is more than 0.98 for treatments of Bare-Fe-Mn, CMC-Fe-Mn and Starch-Fe-Mn, and exhibited a better fitting for the experimental sorption equilibrium data than other isotherm models. In addition, Langmuir isotherm data had higher $R^2$ than Temkin isotherms. In order to assess the potential improvements to $V^{+5}$ removal offered by Fe-Mn nanaparticles over other adsorbents, the Langmuir parameter that has been in most of the previous studies for defining vanadium(V) adsorption capacity of different materials, can be applied to compare the difference of industrial sludge with those of other adsorbents reported in the literature (Table 3).

**Table 3. Comparison of $V^{+5}$ adsorption capacity of Fe-Mn nanoparticle with other adsorbents.**

| **Material** | **Dosage (g/L)** | **qm (mg/g)** | **Citiation** |
|---|---|---|---|
| Bare-Fe-Mn nanopaticle | 0.1 | 129.87 | Current study |
| CMC-Fe-Mn nanoparticle | | 120.48 | Current study |
| Starch-Fe-Mn naoparticle | | 117.65 | Current study |
| $ZnCl_2$ activated sludge carbon | 0.1 | 37.17 | Volkan Doğan & Serdar Aydın ,2014 |
| $ZnCl_2$ activated coir pith carbon | 4 | 24.9 | Namasivayam C and Sangeetha D. 2006 |
| Waste metal sludge | 2 | 24.8 | Bhatnagar,A. etal., 2008 |
| GFH | 1.4 | 111.11 | Naeem,A. etal., 2007 |
| E-33 | 0.5 | 25.06 | |

| | | | |
|---|---|---|---|
| GTO | 2 | 45.66 | |
| Chitosan – Zr(IV) composite | | 208 | Zhang L and Liu X etal.,. 2014 |
| MZ-PPY | 3 | 74.97 | Nomcebo H. etal., 2016 |
| Magnetic Nanoparticles | 38 | 25.71 | Masoome Parijaee, etal , 2014 |

### 3.4 Vanadium absorption characteristic influenced by pH and substrate dosage

The effect of pH was studied by varying the initial pH of $V^{+5}$ solutions within the range of 6–9. Fig.6 shows the pH value effect on CMC-stabilized Fe–Mn particles acting on $V^{+5}$ water. While the solution pH is 6.0, it displayed the highest sorption capacity on the same experimental condition. Therefore, the sorption was favored in lower pH condition. The maximum sorption capacity was observed in pH 6–7, and $V^{+5}$ absorption kinetics model of Fe-Mn nanoparticle belong to pseudo-second-order model (Table 4). However, the uptake dropped sharply at pH > 7, the vanadium adsorption is drop to nearly 20%-30% vanadium absorption amount at pH 8-9 than that in pH 6-7. Absorption effect on heavy metal of pH is very similar with work by B.An and Zhao (2012).

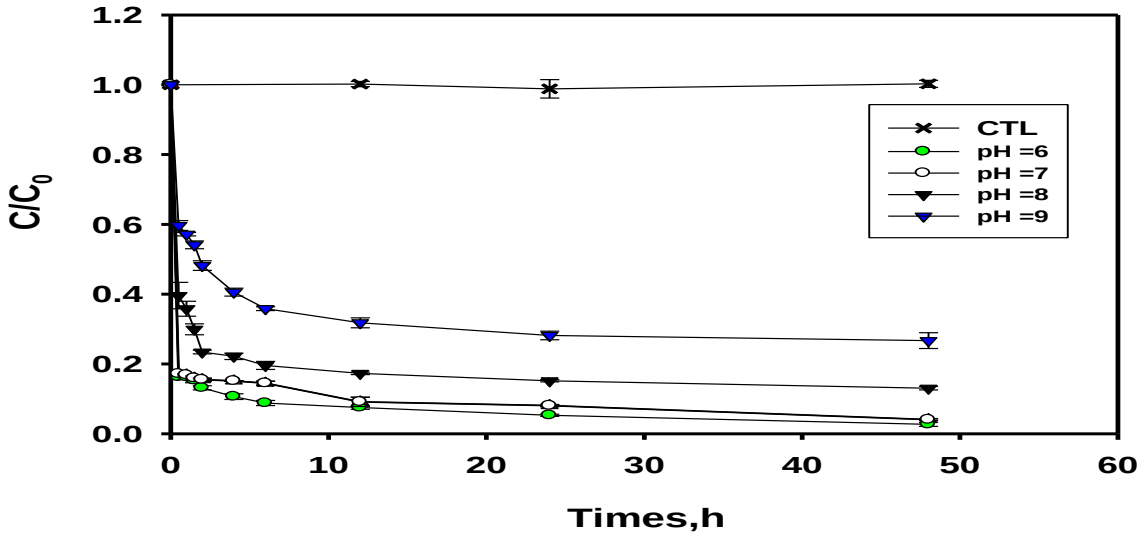

**Fig. 6.** The effect of pH on CMC-stabilized Fe–Mn nanoparticles remove vanadium from water condition. Exp. conditions: Initial V = 10 mg/L, Nanoparticles = 0.1 g/L as Fe, CMC = 0. 1 wt. %, Equilibrium time = 48 h.

**Table 4. Kinetics parameters for $V^{+5}$ adsorption onto CMC-Fe-Mn oxide nanoparticles in different pH conditions.**

| pH | Pseudo-first-order model | | | Pseudo-second-order model | | | Elovich model | | |
|---|---|---|---|---|---|---|---|---|---|
| value | $q_{e\cdot exp}$ (mg/g) | $k_1(h^{-1})$ | $R^2$ | $q_{e\cdot exp}$ (mg/g) | $k_2$(g/mg•h) | $R^2$ | $\alpha$ (g/mg•h) | $\beta$ (g/mg) | $R^2$ |
| pH 6 | 12. 6059 | −0. 1472 | 0. 9318 | **12. 6059** | 0. 2497 | 0. 9998 | 338.5839 | 17.4825 | 0.4462 |
| pH 7 | 12. 4291 | −0. 1758 | 0. 8856 | **12. 4291** | 0. 1968 | 0. 9995 | 6.7871 | 0.5083 | 0.9854 |
| pH 8 | 11. 2634 | −0. 2023 | 0. 8815 | **11. 2634** | 0. 2085 | 0. 9999 | 7.7876 | 0.7311 | 0.9638 |
| pH 9 | 9. 49747 | −0. 1936 | 0. 9615 | **9. 49747** | 0. 1251 | 0. 9998 | 7.7876 | 0.7311 | 0.9638 |

Fig. 7 shows the Bare-Fe-Mn dosage effect on the vanadium adsorption, and Table 5 gives the best-fitted model parameters. The results indicate that the removal rate enhance with increasing material dosage, which is attributed to the increased adsorption sites that are more easily accessible and/or of higher adsorption energy. Based on the $R^2$ value, the pseudo second-order model gives the best data fitting quality. Based on the $k^2$ value, the best remove was observed at the dosage of 0.1 g/L for treating 10 mg/L of $V^{+5}$.

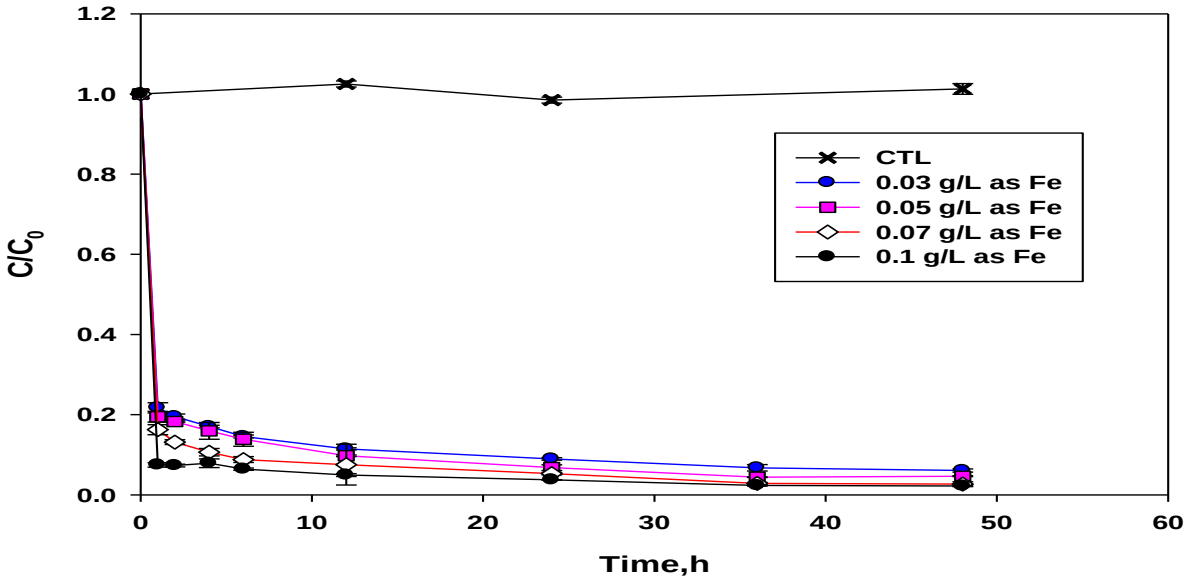


**Fig. 7.** The bare Fe-Mn dosage effect on vanadium adsorption. Exp. conditions: Initial V = 10 mg/L, Nanoparticles = 0.1 g/L as Fe, Equilibrium time = 48 h.

**Table 5. Kinetics parameters for $V^{+5}$ adsorption onto CMC-Fe-Mn oxide nanoparticles in different dosage of Fe-Mn dosage.**

| Dosage of Fe-Mn g/L | Pseudo-first-order model | | | Pseudo-second-order model | | | Elovich model | | |
|---|---|---|---|---|---|---|---|---|---|
| | $q_{e\cdot exp}$ (mg/g) | $k_1(h^{-1})$ | $R^2$ | $q_{e\cdot exp}$ (mg/g) | $k_2$(g/mg•h) | $R^2$ | $\alpha$ (g/mg•h) | $\beta$ (g/mg) | $R^2$ |
| 0.1 | **17.7374** | -0.1224 | 0.9652 | 17.7374 | **17.7374** | 0.9989 | 5.1651 | 0.4965 | 0.9799 |
| 0.07 | **3.1311** | -0.972 | 0.8769 | 3.1311 | **3.1311** | 0.9999 | 58.5657 | 19.9203 | 0.8823 |
| 0.05 | **4.305** | -0.1821 | 0.8049 | 4.305 | **4.305** | 0.9998 | 18.4166 | 5.1626 | 0.9794 |
| 0.03 | **7.0126** | -0.1188 | 0.7319 | 7.0126 | **7.0126** | 0.9997 | 20.7200 | 3.4916 | 0.977 |

### 3.5 The stabilizers concentration effect on removing vanadium.

In order to understand the stabilizer effect on $V^{+5}$ absorption, it is done the work of starch and CMC stabilizer dosage on $V^{+5}$ absorption. The fig.8 expresses equilibrium $V^{+5}$ adsorbed by Fe–Mn nanoparticles with various concentrations of CMC or starch added by 0-0.2 wt. %. Compared to

bare particles, the partially stabilized particles may have inhibited some of the reactive sites, both for thermodynamically and kinetically, which due to the blocking effect of the stabilizer starch or CMC. In contrast, CMC has stronger blocking effect than that of starch. For both stabilizers, further increasing the stabilizer had little further effect on the $V^{+5}$ uptake, it suggested that the gain in adsorption sites due to smaller size is counterbalanced by the formation of a thicker polymer layer on the surface, which slows down the interactions between the nanoparticles and vanadium oxyanions and blocks some of the sorption sites., this is similar with result of Zhao(An and Zhao 2012).

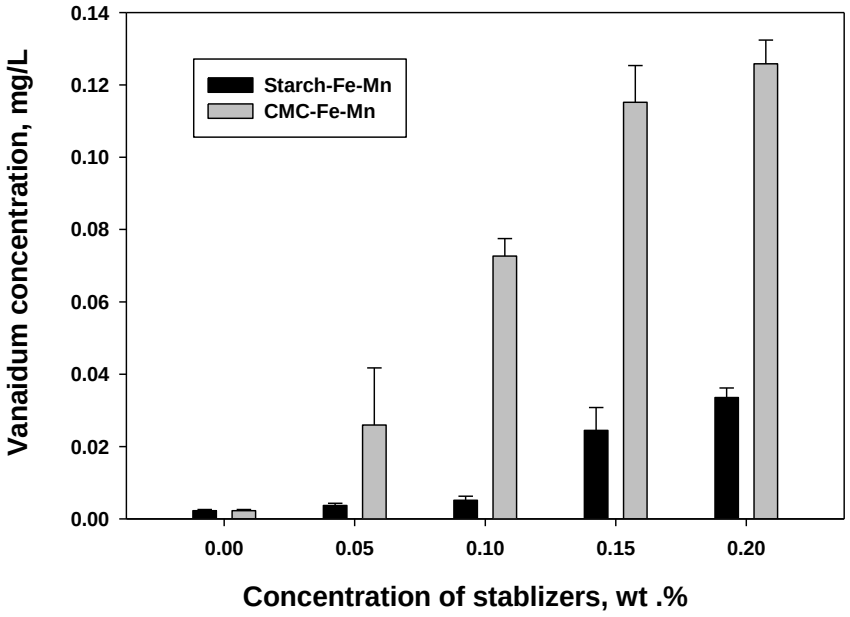


**Fig.8** The stabilizers concentration effect on vanadium adsorption. Exp. conditions: Initial V = 10 mg/L, Nanoparticles = 0.1 g/L as Fe, Stabilizers cons 0-0.2 wt. %: Equilibrium time = 48 h.

**Future work:**

1) Keep studying on Fe-Mn nanoparticles treat vanadium from water with different influencing factor, such as humic acid, temperature and so on.

2) Combine Fe-Mn nanoparticles with different material (zeolite) to produce new method

and material to remove vanadium with high effectivenss.

3) Investigate the treatment effectiveness of stabilize Fe-Mn nanoparticles on removing vanadium from soil, it also may conduct further study on organic.

## 4. Conclusions

This work investigated the vanadium absorption effectiveness of Fe–Mn binary oxide nanoparticles with starch and CMC in stabilizers. The main results are summarized as followings.

Bare Fe-Mn is more capacity for removals $V^{+5}$ than that of starch Fe-Mn and CMC Fe-Mn. Vanadium equilibrium adsorption is the best fit to the Freundlich isotherm for Fe-Mn particles with different stabilizers. Maximum adsorption occurred at pH 7.0, Langmuir isotherm model express that the maximum $V^{+5}$ adsorption capacity was 129.87mg/g, 120.48 mg/g and 117.65 mg/g for bare Fe-Mn CMC Fe-Mn and starch Fe-Mn nanoparticles, respectively.

The Fe–Mn nanoparticles are able to function optimally in range pH 6–7, and significant capacity drop occurs at higher pH condition. Through compared different concentration of stabilizers, it presents that the higher stabilizer concentration may reduce the capacity of removal vanadium from water, it was caused by the stabilizer may block the sorption sites or effect the mass transfer rate. With decreasing the dosage of iron concentration, it will directly reduce Fe-Mn nanoparticle to remove vanadium from water.

The absorption features change are related closely with pre- and post-absorbed surface features, Zeta potential of bare Fe-Mn nanoparticles with different stabilizers, most important is starch and CMC coating the surface of Fe-Mn nanoparicles and decrease the $V^{+5}$ ion adsorption. Therefore, Fe-Mn oxide nanoparticles without stabilizer could be considered as an effective material for treating vanadium pollution in water.

## References:


An, B., Q. Q. Liang, and D. Y. Zhao

2011 Removal of arsenic(V) from spent ion exchange brine using a new class of starch-bridged magnetite nanoparticles. Water Research 45(5):1961-1972.

An, B., and D. Y. Zhao

2012 Immobilization of As(III) in soil and groundwater using a new class of polysaccharide stabilized Fe-Mn oxide nanoparticles. Journal Of Hazardous Materials 211:332-341.

Anirudhan, T. S., and P. G. Radhakrishnan

2010 Adsorptive performance of an amine-functionalized poly(hydroxyethylmethacrylate)-grafted tamarind fruit shell for vanadium(V) removal from aqueous solutions. Chemical Engineering Journal 165(1):142-150.

Arias, M., et al.

2005 Adsorption and desorption of copper and zinc in the surface layer of acid soils. Journal Of Colloid And Interface Science 288(1):21-29.

Ayers, Robert S, and Dennis W Westcot

1985 Water quality for agriculture. Volume 29: Food and Agriculture Organization of the United Nations Rome.

Bellenger, J. P., et al.

2008 Uptake of molybdenum and vanadium by a nitrogen-fixing soil bacterium using siderophores. Nature Geoscience 1(4):243-246.

Bhatnagar, A., et al.

2008 Vanadium removal from water by waste metal sludge and cement immobilization. Chemical Engineering Journal 144(2):197-204.

Deschamps, E., V. S. T. Ciminelli, and W. H. Holl

2005 Removal of As(III) and As(V) from water using a natural Fe and Mn enriched sample.

Water Research 39(20):5212-5220.

Dogan, V., and S. Aydin

2014 Vanadium(V) Removal by Adsorption onto Activated Carbon Derived from Starch Industry Waste Sludge. Separation Science And Technology 49(9):1407-1415.

Goulding, R.

1989 ENVIRONMENTAL-HEALTH CRITERIA-81 - VANADIUM. Journal Of the Royal Society Of Health 109(4):150-151.

He, F., and D. Y. Zhao

2005 Preparation and characterization of a new class of starch-stabilized bimetallic nanoparticles for degradation of chlorinated hydrocarbons in water. Environmental Science & Technology 39(9):3314-3320.

2007 Manipulating the size and dispersibility of zerovalent iron nanoparticles by use of carboxymethyl cellulose stabilizers. Environmental Science & Technology 41(17):6216-6221.

Health, Department of

2010 Healthy lives, healthy people: our strategy for public health in England. Volume 7985: The Stationery Office.

Ho, Y. S., and G. McKay

1998 Sorption of dye from aqueous solution by peat. Chemical Engineering Journal 70(2):115-124.

Imtiaz, M., et al.

2015 Vanadium, recent advancements and research prospects: A review. Environment International 80:79-88.

Juang, R. S., and M. L. Chen

1997 Application of the Elovich equation to the kinetics of metal sorption with solvent-impregnated resins. Industrial & Engineering Chemistry Research 36(3):813-820.

Kavakli, P. A., et al.

2004 Adsorption efficiency of a new adsorbent towards uranium and vanadium ions at low concentrations. Separation Science And Technology 39(7):1631-1643.

Keranen, A., et al.

2015 Removal of nitrate by modified pine sawdust: Effects of temperature and co-existing anions. Journal Of Environmental Management 147:46-54.

Lazaridis, N. K., M. Jekel, and A. I. Zouboulis

2003 Removal of Cr(VI), Mo(VI), and V(V) ions from single metal aqueous solutions by sorption or nanofiltration. Separation Science And Technology 38(10):2201-2219.

Liao, X. P., et al.

2008 Adsorption of metal anions of vanadium(V) and chromium(VI) on Zr(IV)-impregnated collagen fiber. Adsorption-Journal Of the International Adsorption Society 14(1):55-64.

Lim, C. S.

2012 Preparation and characterization of M3V2O8 (M = Ba, Ca) nanoparticles by a MAS method. Journal Of Ceramic Processing Research 13(4):432-436.

Mandiwana, K. L., and N. Panichev

2004 Electrothermal atomic absorption spectrometric determination of vanadium(V) in soil after leaching with Na2CO3. Analytica Chimica Acta 517(1-2):201-206.

Manohar, D. M., B. F. Noeline, and T. S. Anirudhan

2005 Removal of vanadium(IV) from aqueous solutions by adsorption process with aluminum-pillared bentonite. Industrial & Engineering Chemistry Research 44(17):6676-

6684.

Mthombeni, N. H., et al.

2016 Vanadium (V) adsorption isotherms and kinetics using polypyrrole coated magnetized natural zeolite. Journal Of the Taiwan Institute Of Chemical Engineers 66:172-180.

Namasivayam, C., and D. Sangeetha

2006 Removal and recovery of vanadium(V) by adsorption onto ZnCl2 activated carbon: Kinetics and isotherms. Adsorption-Journal Of the International Adsorption Society 12(2):103-117.

Oyewo, O. A., M. S. Onyango, and C. Wolkersdorfer

2017 Adsorptive Performance of Surface-Modified Montmorillonite in Vanadium Removal from Mine Water. Mine Water And the Environment 36(4):628-637.

Parijaee, M., et al.

2014 Adsorption of vanadium(V) from acidic solutions by using octylamine functionalized magnetite nanoparticles as a novel adsorbent. Korean Journal Of Chemical Engineering 31(12):2237-2244.

Parks, J. L., and M. Edwards

2006 Precipitative removal of As, Ba, B, Cr, Sr, and V using sodium carbonate. Journal Of Environmental Engineering-Asce 132(5):489-496.

Peacock, C. L., and D. M. Sherman

2004 Vanadium(V) adsorption onto goethite (alpha-FeOOH) at pH 1.5 to 12: A surface complexation model based on ab initio molecular geometries and EXAFS spectroscopy. Geochimica Et Cosmochimica Acta 68(8):1723-1733.

Peng, H., Z. H. Liu, and C. Y. Tao

2017 Adsorption kinetics and isotherm of vanadium with melamine. Water Science And

Technology 75(10):2316-2321.

Pennesi, C., C. Totti, and F. Beolchini

2013 Removal of Vanadium(III) and Molybdenum(V) from Wastewater Using Posidonia oceanica (Tracheophyta) Biomass. Plos One 8(10).

Qian, S. H., et al.

2004 Studies of adsorption properties of crosslinked chitosan for Vanadium(V), Tungsten(VI). Journal Of Applied Polymer Science 92(3):1584-1588.

Ravishankar, S. A., Pradip, and N. K. Khosla

1995 SELECTIVE FLOCCULATION OF IRON-OXIDE FROM ITS SYNTHETIC MIXTURES WITH CLAYS - A COMPARISON OF POLYACRYLIC-ACID AND STARCH POLYMERS. International Journal Of Mineral Processing 43(3-4):235-247.

Rehder, Dieter

2015 The role of vanadium in biology. Metallomics 7(5):730-742.

Shan, C., and M. P. Tong

2013 Efficient removal of trace arsenite through oxidation and adsorption by magnetic nanoparticles modified with Fe-Mn binary oxide. Water Research 47(10):3411-3421.

Sharififard, H., M. Soleimani, and F. Z. Ashtiani

2017 Optimization of chemical modification process of activated carbon surface with iron nanoparticles for efficient vanadium removal: Kinetics, equilibrium and surface complexation modelling. Desalination And Water Treatment 72:343-353.

Sirvio, J. A., et al.

2016 Bisphosphonate nanocellulose in the removal of vanadium(V) from water. Cellulose 23(1):689-697.

Su, C. M., and D. L. Suarez

1997 In situ infrared speciation of absorbed carbonate on aluminum and iron oxide. Clays And Clay Minerals 45(6):814-825.

Wang, S. C., et al.

2011 Effect of the carboxymethyl chitosan on removal of nickel and vanadium from crude oil in the presence of microwave irradiation. Fuel Processing Technology 92(3):486-492.

Wang, T. G., et al.

2012 The influence of vanadate in calcined Mg/Al hydrotalcite synthesis on adsorption of vanadium (V) from aqueous solution. Chemical Engineering Journal 181:182-188.

Yang, J. Y., et al.

2014 Leaching characteristics of vanadium in mine tailings and soils near a vanadium titanomagnetite mining site. Journal Of Hazardous Materials 264:498-504.

Yeom, B. Y., C. S. Lee, and T. S. Hwang

2009 A new hybrid ion exchanger: Effect of system parameters on the adsorption of vanadium (V). Journal Of Hazardous Materials 166(1):415-420.

Zhang, G. S., et al.

2009 Removal of phosphate from water by a Fe-Mn binary oxide adsorbent. Journal Of Colloid And Interface Science 335(2):168-174.

Zhang, L. F., et al.

2014 Preparation and characterization of chitosan-zirconium(IV) composite for adsorption of vanadium(V). International Journal Of Biological Macromolecules 64:155-161.

Zhang, Y., et al.

2005 Arsenate adsorption on an Fe-Ce bimetal oxide adsorbent: Role of surface properties. Environmental Science & Technology 39(18):7246-7253.